

# On solving the kinematics and controlling of origami box-shaped robots

Phuong Thao Thai<sup>1</sup>, Ngoc Hai Nguyen<sup>2</sup>

<sup>1</sup>Department of Mechatronics, School of Mechanical Engineering, Hanoi University of Science and Technology, Hanoi, Vietnam

<sup>2</sup>VTC Corporation, Hanoi, Vietnam

---

## Article Info

### Article history:

Received Sep 5, 2022

Revised Oct 3, 2022

Accepted Jan 5, 2023

---

### Keywords:

Origami robot

Origami technology

Sarrus linkage

Transformable robot

Waterbomb

---

## ABSTRACT

Nowadays, there is various research on transformable robots. The use of origami patterns for the transformable robot can be found in much research. The disadvantages of the traditional origami model are the suitable material for folding is zero thickness, complicated patterns, and over-constrained mechanism. In this paper, the idea of designing a 1 degree-of-freedom box-shaped robot is proposed and two types of robot design have been analyzed. The first design is the waterbomb robot, which uses the traditional origami pattern. The second model takes the Sarrus linkage as the main mechanism for the mobile robot. In both designs, the transformation of the robot requires only one motor, making the robot lightweight and portable. This paper analyzes the kinematic and dynamic properties of two transformable robots by using MATLAB. The comparison of the torque required for forming a 3D shape has been done for optimizing robot design. Finally, the real model-optimized design is introduced to illustrate the proposed method.

*This is an open access article under the [CC BY-SA](https://creativecommons.org/licenses/by-sa/4.0/) license.*



---

## Corresponding Author:

Phuong Thao Thai

Department of Mechatronics, School of Mechanical Engineering, Hanoi University of Science and Technology

Hanoi, Vietnam

Email: thao.thaihuong@hust.edu.vn

---

## 1. INTRODUCTION

Origami robotics, which is classified as one approach of the transformable robot, is the combination of origami art and robotics with the aim to create robots that can transform into 3D models depending on crease patterns [1]. Robots may effortlessly change their configurations using origami crease patterns with a simple movement. Due to its ability to transform between a 2D and a 3D model in active and sleep modes, origami robots is beneficial for packaging. This versatile feature is an advantage for robots when working in various working spaces. Up to now, there are several studies on robot transformation ability supported by origami art, like miniature origami robots [2], self-folding origami robot [3]–[7], Tribot [8]–[10], and origami-inspired robotic arm [11]–[13]. The idea of making a robot folding origami pattern was investigated in [14], [15]. In these studies, the origami pattern was simplified or made into a series of folding creases, so that the robotic hand was able to fold step-by-step. However, this approach was a little bit time-consuming and required the flexibility of a robot hand. The self-folding robot has been considered in many works, with some material as paper, and alloy [16]. These patterns are connected to each other by using springs or hinges [17] and the robot can jump, and crawl with some actuators.

The most important point that should be considered when making robots from origami patterns is the problem of thickness. Traditional origami pattern is employed on normal paper with zero thickness, whereas the fabric for making the robot is solid to guarantee the strength and stability of the robot. To use origami structures in robots, rigid origami has been considered in much research [18]–[20]. Most research

has recommended thinking about the pattern as a series of interconnected spherical linkages. For instance, thick panels that used tapered surfaces are recommended for folding Miura-ori, meanwhile, others proposed to use offsets at the connection part of panels when folding the square-twist origami pattern. Another research recommended using of cardboard, and the hinges were considered as the first or last layer of the materials. The use of cardboard is suitable for improving the strength of the pattern; however, the use of a hinge is not guaranteed after a long time. Therefore, in this paper, we suggest using origami patterns as a mechanism with polypropylene (PP) material. This material is popular and easy to find when we make real prototypes with 3D printers. The PP material may be difficult to manage with spherical joints, therefore in this paper, we have made the virtual spherical joints by creating holes to prevent collision and have the full function as the original ones.

Inspired by the concept of making a robot from a flat folding pattern [11], the authors of this paper would like to create a mobile box-shaped robot that can transform different shapes with only 1 motor. Therefore, the designing process of this idea is: choosing a suitable 1 degree-of-freedom (DOF) mechanism, kinematics and dynamic analysis, controlling solution, and making a real prototype [21]. We have chosen 2 mechanisms with 1 DOF to analyze 2 designs that are inspired by the Sarrus linkage and waterbomb model. The Sarrus linkage is a mechanical linkage with 1 DOF that can change a circular motion to a linear motion and vice versa [22]. Waterbomb is a traditional origami pattern and has various applications [2], [6]. From the view of rigid origami, the pattern generally has multiple DOFs, but when it is folded symmetrically, the pattern reduces to at least one. Therefore, two designs require just one motor for the transformation of the robot, they are also suitable for making the robot lightweight and portable. In this paper, we investigate the ability to form a process by solving the controlling problem. Then, the necessary torque for this process is calculated and we can base it on the result to make the real prototype.

Compared to previous work about transformable robots and 1 DOF mechanisms, there are some differences between these studies and our research, we have done investigating to carry out the thick origami patterns that are suitable for box-shaped robot transformation, and the kinematics and dynamics are analyzed to derive the equations of motion of the robot so that the robot controlling can be completed. The comparison of the two robot models is also discussed so that researchers can decide which pattern is suitable for making the real prototype.

The rest of the paper is as follows. Section 2 introduces the design of the waterbomb mobile robot and discusses the kinematics and dynamics analysis. The analysis of the Sarrus mobile robot is discussed in section 3. Section 4 consists of the discussion and comparison of two types of mobile robots and the conclusion are written in section 5.

## 2. WATERBOMB ROBOT

### 2.1. Conceptual design of Waterbomb robot

Consider a pattern made by tessellating six-crease waterbomb bases as shown in Figure 1(a). The pattern consists of only two sorts of vertices, D and W, enlarged in Figure 1(b) and (c). The rigid origami folding around each vertex is often modeled kinematically as a spherical 6R linkage in which the creases act as revolute joints and the sheets between creases are rigid links. Generally, a spherical 6R linkage is of three DOFs, but this number is reduced to at least one if only the symmetric folding is allowed [12].

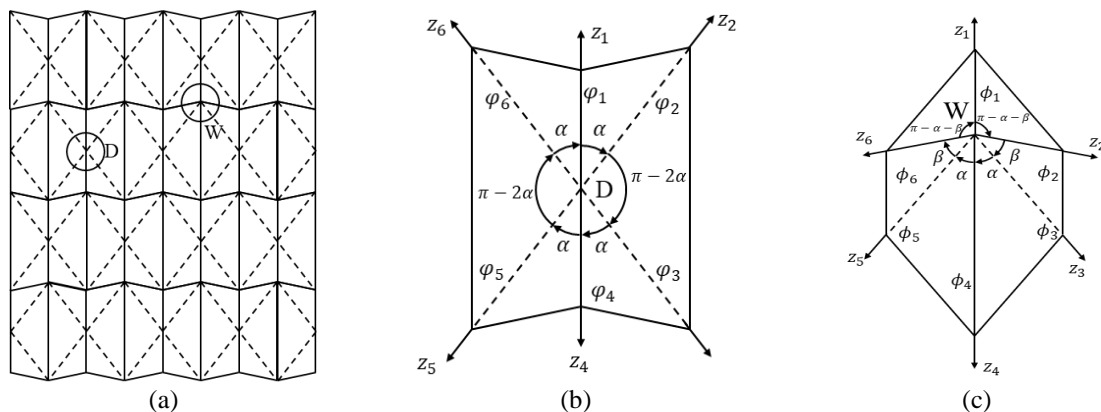


Figure 1. Six-crease waterbomb pattern (a) the general pattern, (b) vertex D and its surrounding creases, (c) vertex W and its surrounding creases

The panels with non-zero thickness can also be folded using the waterbomb tessellation. This is frequently accomplished by mapping the same pattern onto a thick panel while positioning the fold lines on the panel's top or bottom surfaces. Now, at D and W, there will still be sixfold lines in places of creases, but these fold lines do not converge to a vertex. In other words, dissimilar to the zero-thickness sheet, the distances between the adjacent fold lines are no longer zeros. In terms of the kinematic model, the spherical 6R linkage is now replaced by spatial 6R linkages [23], [24]. As shown in Figure 2, the valley and mountain creases remain, and the connection between the creases is almost like hinges. Inspired by the application of waterbomb pattern, a new model of the box-shaped mobile robot has been created. The tessellation pattern of the robot is given in Figure 3(a). In Figure 3(a), there are 6 sides in the box-shaped model. This is a simplified model of waterbomb pattern, only the vertex D and its surrounding creases are used in the new robot model. There are 6 parts for one side of the model, the creases connecting each side with the origami rules can help the model transform a 3D shape into a 2D shape easily. The parameters of the geometric relation are given in Figure 3(b).

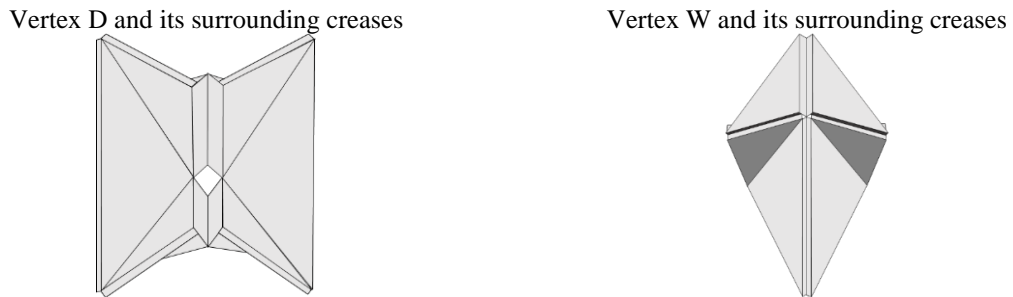


Figure 2. Thick panel model for D and W vertices

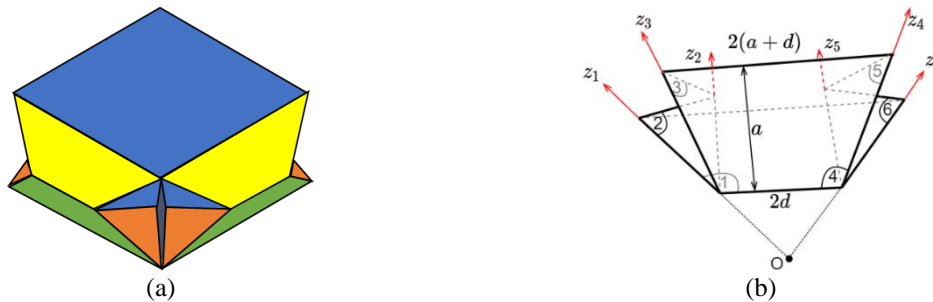


Figure 3. Conceptual design of waterbomb mobile robot (a) the 3D model of waterbomb robot, (b) the geometric parameters of the folding pattern

The thick model of the box is shown in Figure 4. The structure is developed from the tessellation model, the connecting creases used in the thick model are hinges as shown in Figure 4(a). The valley and mountain creases remain in the tessellation as shown in Figures 4(b) and 4(c). However, the thickness of the big parts (purple and cyan parts) is designed double that of 4 four-sided parts (brown, pink, red, and grey parts). The purpose of making a bigger thickness is to create a perfectly flat shape in the sleeping mode of the box as shown in Figures 4(c) and (d).

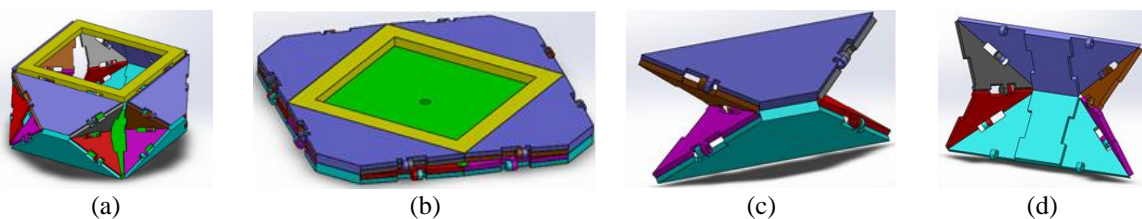


Figure 4. The thick model of waterbomb (a) the box structure of the robot, (b) the flat mode of the box, (c) the folding behavior of one box side, and (d) the inner structure of the box

## 2.2. The kinematics and dynamics analysis

To analyze the kinematic relations of the model, we use the Denavit-Hartenberg method. As the symmetric model, we consider only one side of the box. Panel 1 is the bottom part; the other parts are numbered clockwise. The geometric parameters and the joint angles in valley folds are shown in Figure 5(a). The shapes of mountain folding are given in Figure 5(b). Other D-H parameters are shown in Table 1.

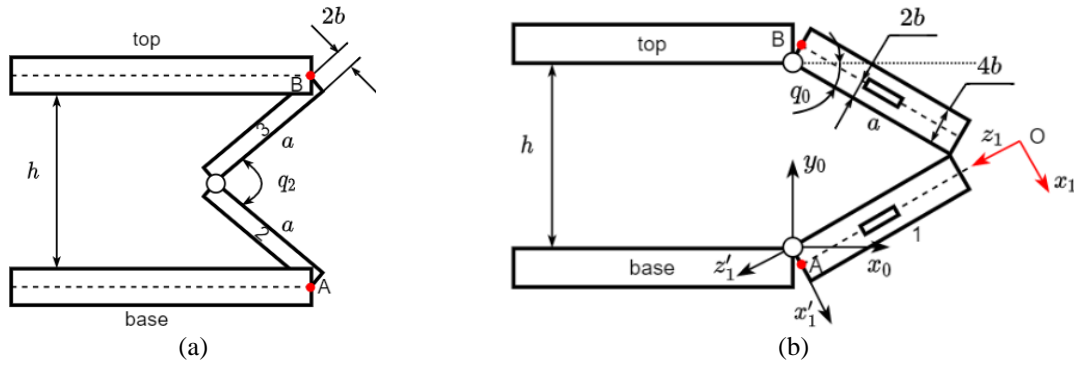


Figure 5. Two folding behaviors of the waterbomb robot (a) valley folding behavior and (b) mountain folding behavior

Table 1. Denavit-Hartenberg parameters of one side of the box-shaped mobile robot

Joint	$\theta_i$	$d_i$	$a_i$	$\alpha_i$
1	$\theta_1$	$d\sqrt{2}$	$2b$	$-\pi/4$
2	$-\theta_2$	0	$-2b$	$-\pi/4$
3	$\theta_3$	$-d\sqrt{2}$	0	$-\pi/2$
4	$\theta_4$	$d\sqrt{2}$	$2b$	$-\pi/4$
5	$-\theta_5$	0	$-2b$	$-\pi/4$
6	$\theta_6$	$-d\sqrt{2}$	0	$-\pi/2$

Let  $q_i$  be the angle between part  $i$  and  $i + 1$ , therefore, with mountain crease:  $q_i = \pi - \theta_i$ , and with valley crease  $q_i = \pi + \theta_i$ . As the model is symmetric, then  $q_1 = q_6 = q_3 = q_4$ ;  $q_2 = q_5$ . The relation between  $q_1$  and  $q_2$  is given as (1).

$$\tan \frac{q_2}{2} = \sqrt{2} \tan \frac{q_1}{2} \quad (1)$$

As can be seen in the Figure 5(a), we can derive:

$$h = 2a \sin q_0 \Rightarrow AB = 2a \sin \frac{q_2}{2} + 2.2b \cos \frac{q_2}{2} = 2a \sin q_0 + 2.2b \cos q_0 \Rightarrow q_2 = 2q_0 \quad (2)$$

The transformation matrix is calculated as:

$$T_{01} = \begin{bmatrix} 1 & 0 & 0 & -2b \\ 0 & 1 & 0 & - \\ 0 & 0 & 1 & -(a+d)\sqrt{2} \\ 0 & 0 & 0 & 1 \end{bmatrix} \quad (3)$$

The position of mass center is determined as:

$$\begin{aligned} p_{C_1}^0 &= T_{01} [b \quad \dots \quad \dots \quad 1]^T = [x_{C_1} \quad y_{C_1} \quad z_{C_1} \quad 1]^T \\ p_{C_2}^0 &= T_{02} T_{12} [-b \quad \dots \quad \dots \quad 1]^T = [x_{C_2} \quad y_{C_2} \quad z_{C_2} \quad 1]^T \\ p_{C_3}^0 &= T_{01} T_{12} T_{23} [b \quad \dots \quad \dots \quad 1]^T = [x_{C_3} \quad y_{C_3} \quad z_{C_3} \quad 1]^T \end{aligned}$$

$$p_{C_4}^0 = [x_{C_1} \quad h - y_{C_1} \quad z_{C_1} \quad 1]^T; p_{C_5}^0 = [x_{C_3} \quad y_{C_3} \quad -2a - 2d - z_{C_3} \quad 1]^T$$

$$p_6^0 = [x_{C_2} \quad y_{C_2} \quad -2a - 2d - z_{C_2} \quad 1]^T$$

Let  $r_{C_i} = [x_{C_i} \quad y_{C_i} \quad z_{C_i}]$ ,  $q = [q_0 \quad q_1]^T$ , the kinetic energy of 2 big plates is calculated as (4),

$$2T = 2J_{big}\dot{q}_0^2 + \sum_{i=1,4} m_i \dot{r}_{C_i}^T \dot{r}_{C_i} = \dot{q}^T \left( \sum_{i=1,4} m_i J_{T_{C_i}}^T J_{T_{C_i}} \right) \dot{q} + \dot{q}^T \begin{bmatrix} 2J_{big} & 0 \\ 0 & 0 \end{bmatrix} \dot{q} \quad (4)$$

in which,  $J_{big}$  is the mass moment of inertia of 2 big plates around its shafts. The kinetic energy of 4 small plates is calculated as (5).

$$2T = \sum_{i=2,3,5,6} (m_i \dot{r}_{C_i}^T \dot{r}_{C_i} + w_i^T I_{C_i} w_i) \quad (5)$$

in which,  $w_2 = [\omega_{x2} \quad \omega_{y2} \quad \omega_{z2}]$ ,  $w_6 = [-\omega_{x2} \quad -\omega_{y2} \quad \omega_{z6}]$ ;

$$w_3 = [\omega_{x3} \quad \omega_{y3} \quad \omega_{z3}], \quad w_5 = [-\omega_{x3} \quad -\omega_{y3} \quad \omega_{z3}]$$

$$I_{C3} = I_{C6} = \begin{bmatrix} J_1 & 0 & 0 \\ 0 & J_2 & 0 \\ 0 & 0 & J_3 \end{bmatrix}, I_{C2} = I_{C5} = \begin{bmatrix} J_1 & 0 & 0 \\ 0 & (J_2 + J_3)/2 & (J_3 - J_2)/2 \\ 0 & (J_3 - J_2)/2 & (J_2 + J_3)/2 \end{bmatrix} \quad (6)$$

Kinetic energy of 1 side of waterbomb model is derived as (7).

$$T = 0.5\dot{q}^T \left( \sum_{i=1,6} m_i J_{T_{C_i}}^T J_{T_{C_i}} + \begin{bmatrix} 2I_{big} & 0 \\ 0 & 0 \end{bmatrix} + \sum_{i=2,3,5,6} J_{R_i}^T I_{C_i} J_{R_i} \right) \dot{q} \quad (7)$$

Hence,

$$M_S(q) = \sum_{i=1,6} m_i J_{T_{C_i}}^T J_{T_{C_i}} + \begin{bmatrix} 2I_{big} & 0 \\ 0 & 0 \end{bmatrix} + \sum_{i=2,3,5,6} J_{R_i}^T I_{C_i} J_{R_i} \quad (8)$$

Kinetic energy of the top part:

$$T = 0.5m_t \dot{h}^2 \quad (9)$$

Hence,

$$M_t(q) = m_t \begin{bmatrix} (2a \cos q_0 - 4b \sin q_0)^2 & 0 \\ 0 & 0 \end{bmatrix} \quad (10)$$

$$G_t(q) = m_t g \begin{bmatrix} 2a \cos q_0 - 4b \sin q_0 \\ 0 \end{bmatrix} \quad (11)$$

Then, we derive (12).

$$M(q) = 2M_S + M_t; G(q) = 2G_S + G_t; C(q, \dot{q}) \quad (12)$$

The motion of the waterbomb robot is derived as (13).

$$M(q)\ddot{q} + C(q, \dot{q})\dot{q} + G(q) + A^T \lambda = U \quad (13)$$

The linkage equation is as (14).

$$f = \tan q_0 - \sqrt{2} \tan \frac{q_1}{2} = 0 \quad (14)$$

Hence,

$$A = \left[ \tan^2 q_0 + 1 \quad -\frac{\sqrt{2}}{2} (\tan^2 \frac{q_1}{2} + 1) \right] \Rightarrow A\dot{q} = 0 \Rightarrow A\ddot{q} + \dot{A}\dot{q} = 0 \quad (15)$$

Then motion of the robot is derived as in (13). From (1) and (2), we derive (16) and (17).

$$\dot{q}_1 = \frac{\dot{q}_0(\tan^2 q_0 + 1)}{\frac{\sqrt{2}}{2}(\tan^2 \frac{q_1}{2} + 1)} = \frac{2\dot{q}_0(\tan^2 q_0 + 1)}{\sqrt{2}(\tan^2 q_0 + 1)} \quad (16)$$

$$\ddot{q}_1 = \frac{2(\ddot{q}_0 + 2\dot{q}_0 \tan q_0)(\tan^2 q_0 + 1) - \frac{\dot{q}_1^2}{2}(\tan q_0)(\tan^2 q_0 + 2)}{\sqrt{2}(\tan^2 q_0 + 2)} \quad (17)$$

### 2.3. Control of waterbomb robot

The PD control torque is computed as (18),

$$U = M(q)(\ddot{q}_d + K_d \dot{e} + K_p e) + C(q, \dot{q})\dot{q} + G(q) \quad (18)$$

in which,  $e = q - q_d$ ,  $q_d$  is the desired angle. The motion of the desired angle is designed as in Table 2. The PD control parameters in the simulation are given as  $K_p = 900$ ,  $K_d = 60$ . The total mass of the model designed on SolidWorks is 1768 g and the area of the model at flat mode is calculated as (19).

$$200 \times 200 + 4 \times (200 + 50) \div 2 \times 75 = 0.775.10^6 (mm^2) \quad (19)$$

The results of this controllation are given in Figure 6. As can be seen in this figure, after 2 seconds, the constant trajectory is depicted in Figure 6(a). The error of controllation and the computed torque are illustrated in Figures 6(b) and 6(c). The figures show that these input actuation histories can be quite large when the gains are large. The reason we choose the controllation trajectory is the quadratic equation to form the 3D shape, if we choose the position equation, the singularity may occur and reduce the strength of the mechanism.

Table 2. Designed trajectory for controlling

Time	Desired angle (degree)
0s-1s	0.01
1s-2s	$q_d(t) = 0.01 + 269.94(t-1)^2 - 179.96(t-1)^3$ $\Delta t = 0.001s$
2s-3s	89.99

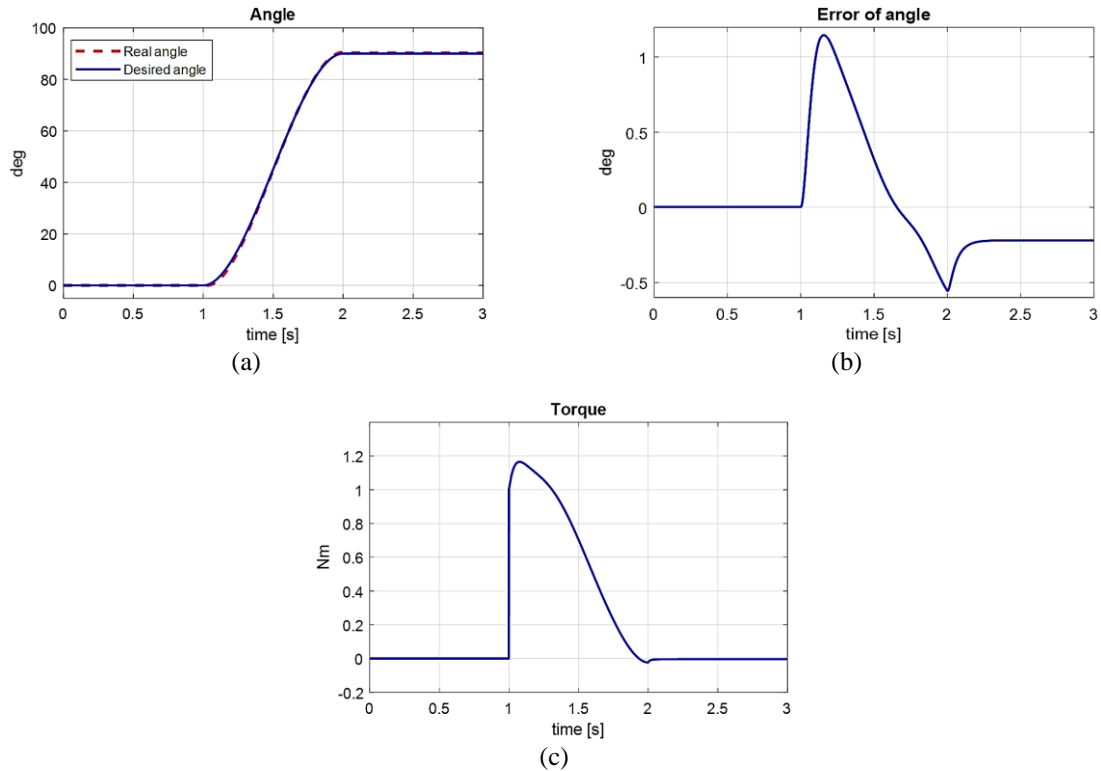


Figure 6. Results of PD controlling with trajectory: (a) result of controlling angle, (b) error of angle during controlling time, and (c) result of controlling torque

### 3. SARRUS ROBOT

#### 3.1. Conceptual design of Sarrus robot

With the idea of creating a robot that can transform from 2D to 3D, the 3D configuration, also known as “cubic mode” or “active mode”, should have the shape of a box with wheels. Meanwhile, in the 2D configuration, also known as “flat mode” or “sleep mode”, the wheels are hidden, and two Sarrus linkages are combined. The schematic design of the first and second linkage is illustrated in Figures 7(a) and 8(a), and the full model design is illustrated respectively in Figures 7(b) and 8(b).

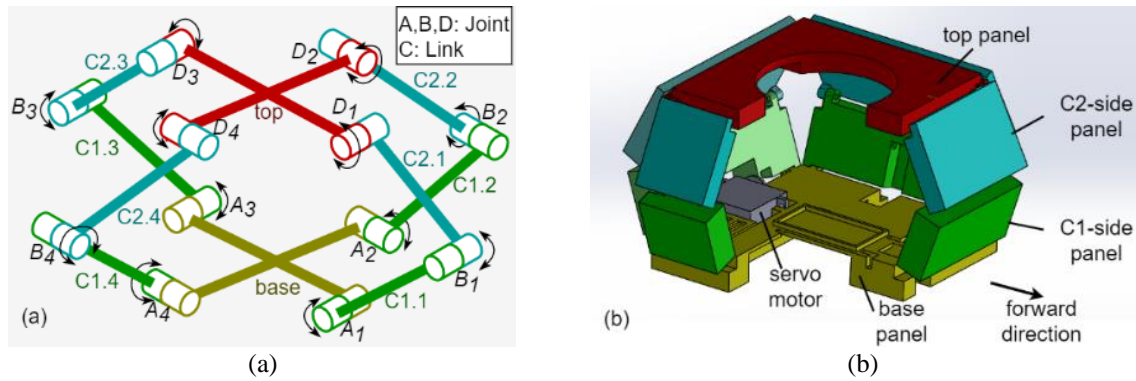


Figure 7. The design of (a) the schematic of the first Sarrus linkage and (b) the linkage

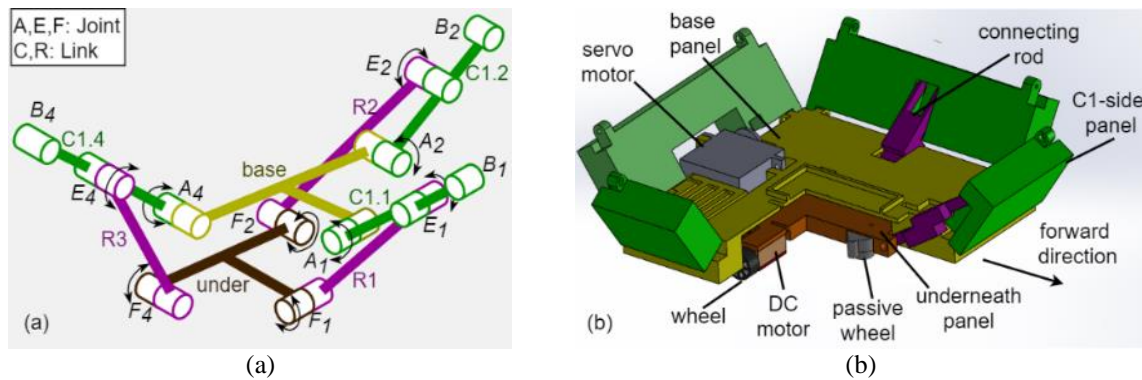


Figure 8. The design of (a) the schematic of the second Sarrus linkage and (b) the linkage

The main body of the robot in active mode is formed by the first linkage, a four-sided Sarrus linkage, as shown in Figures 7(a) and 7(b). There is one based panel where the motor for transformation is mounted on. Four pairs of panels connect four sides of the base panel and those of the top panel. There are two types of side panels: the below-sided panel called the C1-side panel and the upper one called the C2-side panel. The sizes of the side panels are equal to satisfy the condition of a Sarrus linkage. All the joints are revolute joint. The motor directly controls only one of them, while the other joints are passive joints.

The second linkage as shown in Figures 8(a) and 8(b) is a variant of Sarrus linkage which let an underneath panel with wheels move down during transformation into active mode. The base panel and three C1-side panels adjacent to the base panel are shared by the two Sarrus linkages. To accommodate the three connections that complete the second Sarrus linkage, cuts are created in the base panel. The active joint is not a part of the second Sarrus linkage to save space for the motor for transformation. The sizes of wheels should be small enough to be hidden in the flat mode.

In the active mode, three wheels (two active wheels controlled by two DC motors and one passive wheel for navigation) are activated as they touch the ground. Table 3 shows the basic parameters of the Sarrus mobile robot, while Figure 9 illustrates our design in 2 modes: flat mode in Figure 9(a) and cubic mode in Figure 9(b). Figure 10 shows the prototype of the double Sarrus. The prototype is created using 3D printers, the material is PP plastic.

Table 3. Parameters of Sarrus mobile robot

Robot parameters		Description
Robot	Dimensions in flat mode	256x256x36 mm
	Dimensions in 3D mode	180x180x148 mm
	Mass	1500 g
Actuator	Material	Polylactic Acid
	Transformable mechanism	1 servo motor
	Mobile mechanism	2 DC servo motors
Control	Main controller	Arduino pro mini
	Power	2 LiPo batteries DC 3.7 V

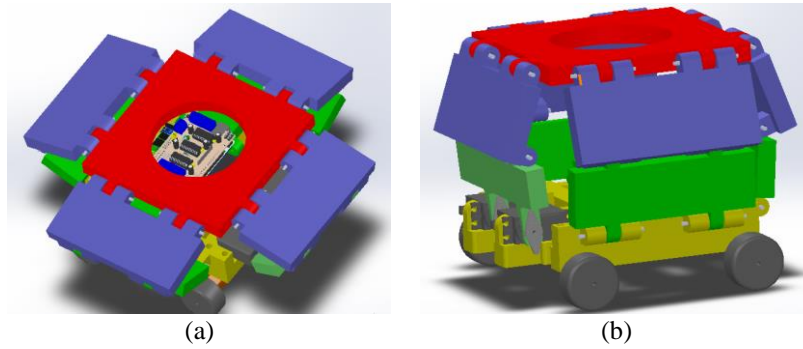


Figure 9. Flat and cubic mode of Sarrus mobile robot (a) flat mode and (b) cubic mode

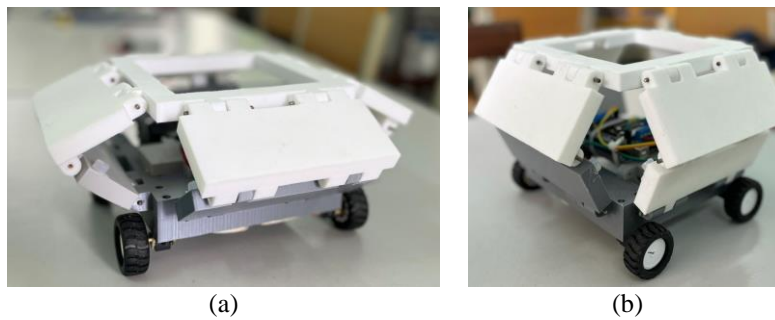


Figure 10. The prototype of Sarrus mobile robot (a) flat mode and (b) cubic mode

### 3.2. Analysis of kinematics and dynamics

A dynamic model has been created to analyze the movement of transforming. Figure 11 illustrates the kinematic parameters, variables, and coordinate system. Table 4 gives the dynamic parameters.

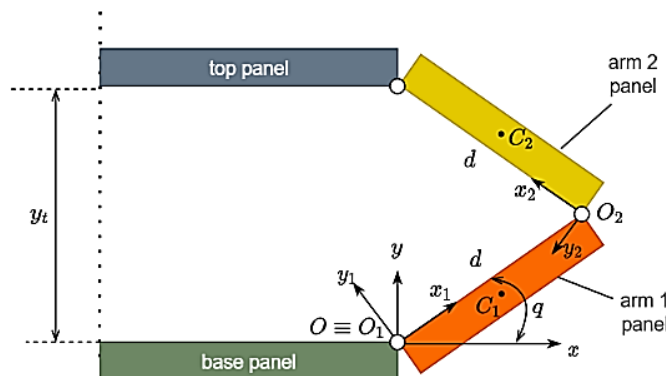


Figure 11. Dynamic model



Table 4. Dynamic parameters of double-Sarrus mobile robot

Symbol	Description
$m_t$	Mass of top panel
$m_{cm}$	Mass of arm motor
$m_{c1}$	Mass of arm 1 panel
$m_{c2}$	Mass of arm 2 panel
$I_{cm}$	Inertia moment of arm motor
$I_{c1}$	Inertia moment of arm 1 panel
$I_{c2}$	Inertia moment of arm 2 panel
$m_t$	Mass of top panel

When moving, the kinematics coordinates are connected by (20) to (26).

$$y_t - 2d \sin q = 0 \quad (20)$$

$$x_{c1} = a_1 \cos q - b_1 \sin q \quad (21)$$

$$y_{c1} = a_1 \sin q + b_1 \cos q \quad (22)$$

$$x_{cm} = a_m \cos q - b_m \sin q \quad (23)$$

$$y_{cm} = a_m \sin q + b_m \cos q \quad (24)$$

$$x_{c2} = d \cos q - a_2 \cos q + b_2 \sin q \quad (25)$$

$$y_{c2} = d \sin q + a_2 \sin q + b_2 \cos q \quad (26)$$

Kinetics and potential energy are calculated as (27) and (28).

$$T = \frac{1}{2} \cdot 3(m_{c1} v_{c1}^2 + I_{c1} \dot{q}^2) + \frac{1}{2} \cdot 4(m_{c2} v_{c2}^2 + I_{c2} \dot{q}^2) + \frac{1}{2}(m_{cm} v_{cm}^2 + I_{cm} \dot{q}^2) + \frac{1}{2} m_t v_t^2 \quad (27)$$

$$\Pi = g(3m_{c1} y_{c1} + 4m_{c2} y_{c2} + m_{cm} y_{cm} + m_t y_t) \quad (28)$$

The general form of equation of motion is given as (29),

$$U = M(q)\ddot{q} + C(q, \dot{q})\dot{q} + G(q) \quad (29)$$

in which,

$$M(q) = 3m_{c1} \left( \left( \frac{\partial x_{c1}}{\partial q} \right)^2 + \left( \frac{\partial y_{c1}}{\partial q} \right)^2 \right) + 4m_{c2} \left( \left( \frac{\partial x_{c2}}{\partial q} \right)^2 + \left( \frac{\partial y_{c2}}{\partial q} \right)^2 \right) + m_{cm} \left( \left( \frac{\partial x_{cm}}{\partial q} \right)^2 + \left( \frac{\partial y_{cm}}{\partial q} \right)^2 \right) + m_t \left( \frac{\partial y_t}{\partial q} \right)^2 + (3I_{c1} + 4I_{c2} + I_{cm}) \quad (30)$$

$$C(q, \dot{q})\dot{q} = \frac{1}{2} \frac{\partial M(q)}{\partial q} \dot{q}^2 \quad (31)$$

$$G(q) = g \left( 3m_{c1} \frac{\partial y_{c1}}{\partial q} + 4m_{c2} \frac{\partial y_{c2}}{\partial q} + m_{cm} \frac{\partial y_{cm}}{\partial q} + m_t \frac{\partial y_t}{\partial q} \right) \quad (32)$$

### 3.3. Control and simulation

#### 3.3.1. Transformation

The PD control torque is computed as (33),

$$U = M(q)(\ddot{q}_d + K_d \dot{e} + K_p e) + C(q, \dot{q})\dot{q} + G(q) \quad (33)$$

in which  $e = q_d - q$ ,  $q_d$  is the desired angle. The motion of the desired angle is designed as in Table 5. The PD control parameters in the simulation are given as  $K_d = 200$ ,  $K_p = 10000$ . The simulation has been

completed with a quadratic trajectory as shown in Figure 12. After 1 second, the 3D structure of the robot is formed, and the torque needed for the forming process is 1.2 Nm.

Table 5. The motion of desired angle

Time	Desired angle (degree)
0s–0.5s	0
0.5s–1.5s	$q_d(t) = 0,01 + 269,94(t - 1)^2 - 179,96(t - 1)^3$ $\Delta t = 0,001s$
1.5s–2s	90

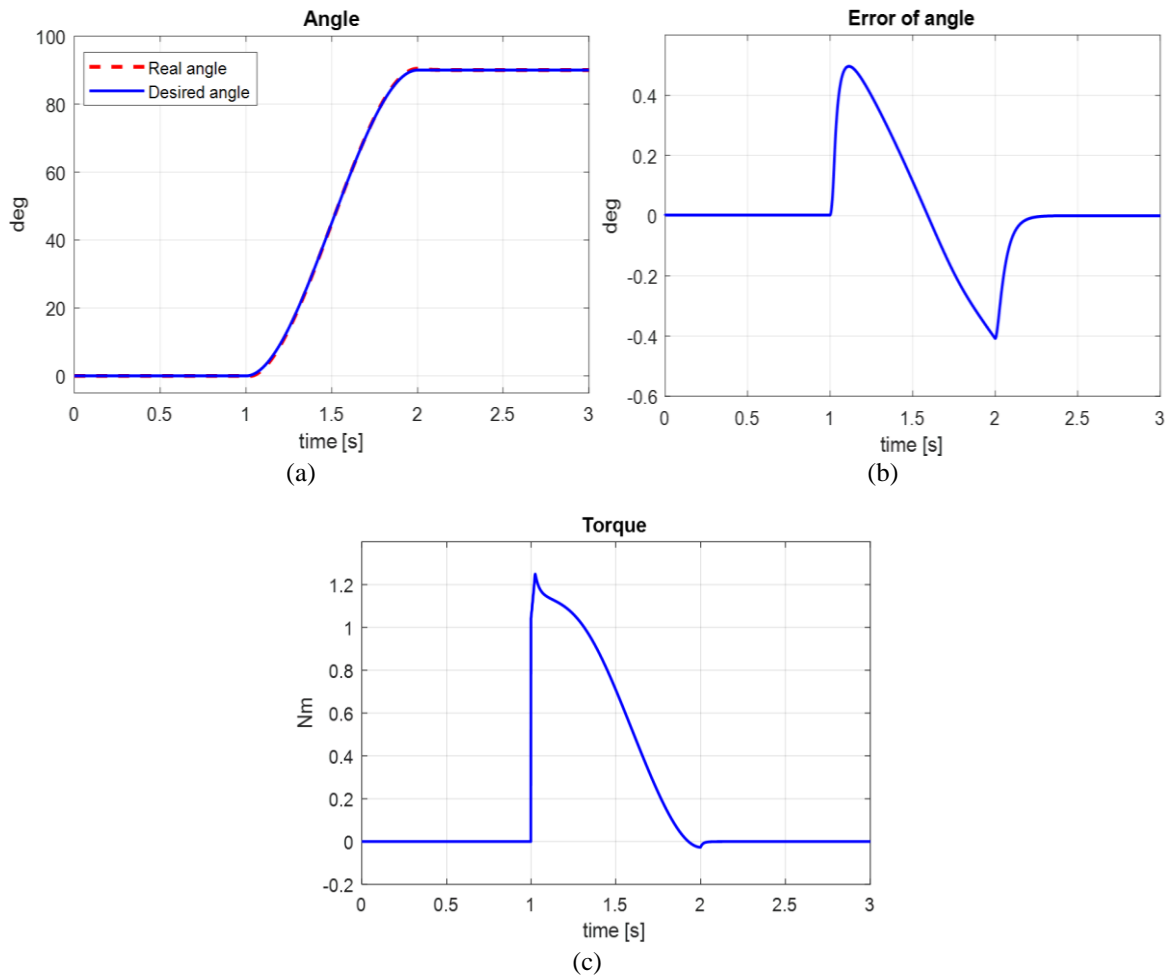


Figure 12. Results of PD controlling with trajectory (a) result of controlling angle, (b) error of angle during controlling time, and (c) result of controlling torque

### 3.3.2. Mobility

The control system has a joystick on the smartphone, a Bluetooth module HC05, an Arduino pro mini microcontroller, two DC motors, a DC motor driver L293D, and two LiPo power batteries. The joystick position is sent to the Arduino via the Bluetooth module. Then, the Arduino program processes and sends pulse width modulation (PWM) to the DC motor driver. The PWM signal is converted into a voltage applied to the two DC motors. The movements of the robot are controlled by Arduino UNO. The control program takes some basic moving: going straight, going backward, turning left or right, lifting, or putting down [25]. The Bluetooth signal transfers from a smartphone to Arduino and the robot will be taken programmed action.

The application will send a signal of the joystick's position through Bluetooth when the joystick on the phone is dragged. The joystick position is given by x-y coordinates with a value from 0 to 255. The Arduino will receive the signal then process it using the control algorithm, and a PWM value from -255 to

255 will be sent to the motors. Positive values are associated with forward motion and vice versa. Details can be found in Figures 13 and 14.

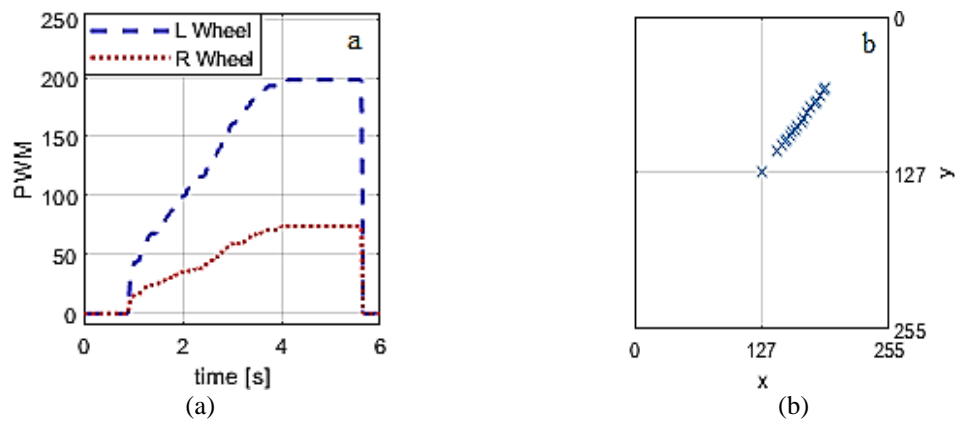


Figure 13. Results of mobility controlling (a) PWM for two wheels when moving forward to the right and (b) the joystick position

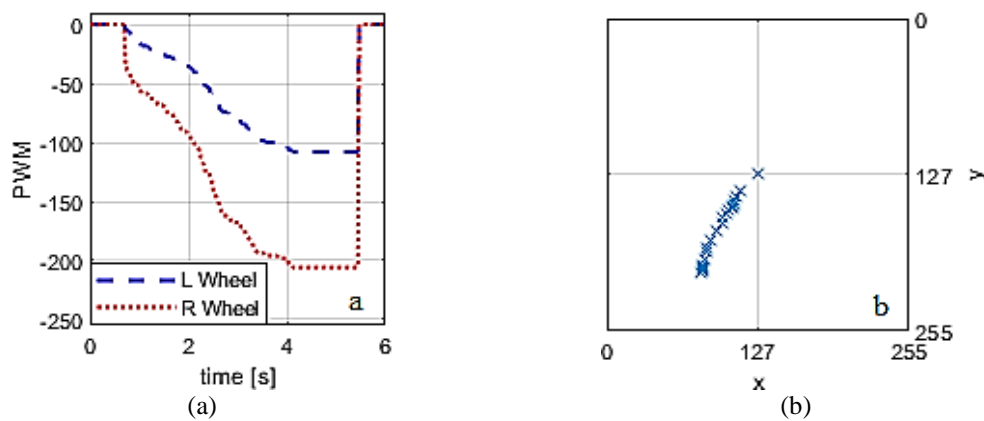


Figure 14. Results of mobility controlling (a) PWM for two wheels when moving backward to the right and (b) the joystick position

#### 4. DISCUSSION AND COMPARISON

To compare and then optimize the design of a transformable box-shaped robot, we have made two robot types with the same size, same material, and same mass. First, we discuss the mechanism complication. The waterbomb robot consists of 6 parts on one side, while there are 2 parts on one side of the Sarrus mobile robot. Apparently, the mechanism of the Sarrus mobile robot is not as complicated as the waterbomb robot. There are only 2 parts on each side of Sarrus robot, whereas, in waterbomb model, the number of parts on one side is 6. Waterbomb is the traditional origami pattern, it consists of origami properties then the design of waterbomb robot is the same as the original one. As we manage to design with thick panels, then the design is simpler, however, the mechanism is much more complicated than the Sarrus mobile. The Sarrus linkages are easier to make real prototypes. After the kinematics and dynamics have been analyzed, we calculated the torques that are necessary for the forming process of the two mobile robots. As in Table 6, with the same size and approximately the same mass, the torque is approximately the same. However, the error of the desired angle of the Sarrus mobile robot is less than waterbomb mobile robot. The maximum error angle in Sarrus mobile robot is 0.4 degrees, whereas in waterbomb design is 1 degree. Therefore, we choose the model of Sarrus mobile robot for creating the real model. The necessary torque for forming process is 1.2 (Nm), which is the same as the simulation. The mobility of the real model of Sarrus mobile has been verified and received good results as designed.

For future works, the model can be developed with several purposes for packaging and working in harsh environments. The speed of forming a 3D structure should be fastened to be suitable for working

conditions. As can be seen in the real model, the forming process takes more time than 5 seconds. The reason for this problem may be due to 3D printing errors and the friction between links and joints of the mechanism.

Table 6. Comparison of two box-shaped robots

	Waterbomb robot	Sarrus robot
Mass	1768 g	1773,64 g
Number of parts of 1 side	6 parts	2 parts
Dimension	$0,775.10^6 mm^2$	$1.10^6 mm^2$
Calculated torque	1.11 Nm	1.23 Nm
Error of angle	1.03 deg	0.45 deg

## 5. CONCLUSIONS

This research aims to apply a new mechanism inspired by origami patterns for the mobile box-shaped robots to form a 3D shape form from the 2D model with only 1 motor. Two models have been implemented in this paper: the Sarrus linkage and waterbomb pattern. The kinematics and kinetics are analyzed and applied to the problem of controlling, then the desired 3D shape of the mobile robot is formed. The value of driving torque for forming the mechanism has been calculated by MATLAB. The comparison of the two models has been discussed and the authors have found out the optimized design for the box-shaped robot with the requirement of lightweight and 1 DOF. The real model of the Sarrus mobile robot has been completed by a 3D printer. In future research, the problem of improving forming speed and accuracy should be considered carefully.

## ACKNOWLEDGEMENTS

This research is funded by Hanoi University of Science and Technology (HUST) under project number T2021-SAHEP-010.




## REFERENCES

- [1] K. Kuribayashi *et al.*, "Self-deployable origami stent grafts as a biomedical application of Ni-rich TiNi shape memory alloy foil," *Materials Science and Engineering: A*, vol. 419, no. 1–2, pp. 131–137, Mar. 2006, doi: 10.1016/j.msea.2005.12.016.
- [2] C. D. Onal, R. J. Wood, and D. Rus, "An origami-inspired approach to worm robots," *IEEE/ASME Transactions on Mechatronics*, vol. 18, no. 2, pp. 430–438, Apr. 2013, doi: 10.1109/TMECH.2012.2210239.
- [3] B. An and D. Rus, "Designing and programming self-folding sheets," *Robotics and Autonomous Systems*, vol. 62, no. 7, pp. 976–1001, Jul. 2014, doi: 10.1016/j.robot.2013.06.015.
- [4] T. Tachi, "Rigid-foldable thick origami," in *Origami 5*, A K Peters/CRC Press, 2011, pp. 253–263. doi: 10.1201/b10971-24.
- [5] J. Kim, D.-Y. Lee, S.-R. Kim, and K.-J. Cho, "A self-deployable origami structure with locking mechanism induced by buckling effect," in *2015 IEEE International Conference on Robotics and Automation (ICRA)*, May 2015, pp. 3166–3171. doi: 10.1109/ICRA.2015.7139635.
- [6] S. M. Felton, M. T. Tolley, C. D. Onal, D. Rus, and R. J. Wood, "Robot self-assembly by folding: A printed inchworm robot," in *2013 IEEE International Conference on Robotics and Automation*, May 2013, pp. 277–282. doi: 10.1109/ICRA.2013.6630588.
- [7] M. T. Tolley, S. M. Felton, S. Miyashita, D. Aukes, D. Rus, and R. J. Wood, "Self-folding origami: shape memory composites activated by uniform heating," *Smart Materials and Structures*, vol. 23, no. 9, Sep. 2014, doi: 10.1088/0964-1726/23/9/094006.
- [8] B. J. Edmondson, R. J. Lang, S. P. Magleby, and L. L. Howell, "An offset panel technique for thick rigidly foldable origami," *Aug. 2014*. doi: 10.1115/DETC2014-35606.
- [9] Z. Zhakypov, C. H. Belke, and J. Paik, "Tribot: A deployable, self-righting and multi-locomotive origami robot," in *2017 IEEE/RSJ International Conference on Intelligent Robots and Systems (IROS)*, Sep. 2017, pp. 5580–5586. doi: 10.1109/IROS.2017.8206445.
- [10] C. H. Belke and J. Paik, "Automatic couplings with mechanical overload protection for modular robots," *IEEE/ASME Transactions on Mechatronics*, vol. 24, no. 3, pp. 1420–1426, Jun. 2019, doi: 10.1109/TMECH.2019.2907802.
- [11] J. S. Ku and E. D. Demaine, "Folding flat crease patterns with thick materials," *Journal of Mechanisms and Robotics*, vol. 8, no. 3, Jun. 2016, doi: 10.1115/1.4031954.
- [12] Y. Chen, H. Feng, J. Ma, R. Peng, and Z. You, "Symmetric waterbomb origami," *Proceedings of the Royal Society A: Mathematical, Physical and Engineering Sciences*, vol. 472, no. 2190, p. 20150846, Jun. 2016, doi: 10.1098/rspa.2015.0846.
- [13] P. T. Thai and N. N. Hai, "Design and control of a double-Sarrus mobile robot," in *Advances in Asian Mechanism and Machine Science*, Springer International Publishing, 2022, pp. 269–278. doi: 10.1007/978-3-030-91892-7\_25.
- [14] P. T. Thai, M. Savchenko, H. T. T. Nguyen, and I. Hagiwara, "Simulation-based approach for paper folding with the aim to design the origami-performing robotic system," *Mechanical Engineering Journal*, vol. 3, no. 6, 2016, doi: 10.1299/mej.15-00668.
- [15] P. T. Thai, M. Savchenko, and I. Hagiwara, "Finite element simulation of robotic origami folding," *Simulation Modelling Practice and Theory*, vol. 84, pp. 251–267, May 2018, doi: 10.1016/j.simpat.2018.03.004.
- [16] J. K. Paik and R. J. Wood, "A bidirectional shape memory alloy folding actuator," *Smart Materials and Structures*, vol. 21, no. 6, Jun. 2012, doi: 10.1088/0964-1726/21/6/065013.





- [17] C. Nara, I. Hagiwara, Y. Yang, and X. Chen, "Flat-foldable boxes of thick panels: hinges and supportors," 2017.
- [18] T. Tachi, "Simulation of rigid origami," *Origami*, vol. 4, no. 8, pp. 175–187, 2009.
- [19] H. Feng, R. Peng, J. Ma, and Y. Chen, "Rigid foldability of generalized triangle twist origami pattern and its derived 6R linkages," *Journal of Mechanisms and Robotics*, vol. 10, no. 5, Oct. 2018, doi: 10.1115/1.4040439.
- [20] Y. Chen, R. Peng, and Z. You, "Origami of thick panels," *Science*, vol. 349, no. 6246, pp. 396–400, Jul. 2015, doi: 10.1126/science.aab2870.
- [21] T. Tachi and G. Epps, "Designing one-DOF mechanisms for architecture by rationalizing curved folding," in *International Symposium on Algorithmic Design for Architecture and Urban Design (ALGODE-AIJ)*. Tokyo, 2011, pp. 1–6.
- [22] T. Koetsier and M. Ceccarelli, Eds., *Explorations in the History of Machines and Mechanisms*, vol. 15. Dordrecht: Springer Netherlands, 2012. doi: 10.1007/978-94-007-4132-4.
- [23] Y. Chen and Z. You, "Two-fold symmetrical 6R foldable frame and its bifurcations," *International Journal of Solids and Structures*, vol. 46, no. 25–26, pp. 4504–4514, Dec. 2009, doi: 10.1016/j.ijsolstr.2009.09.012.
- [24] H. Feng, "Kinematics of spatial linkages and its applications to rigid origami," Université Clermont Auvergne, 2018.
- [25] İ. Mertiyüz, A. K. Tanyıldızı, B. Taşar, A. B. Tatar, and O. Yakut, "FUHAR: A transformable wheel-legged hybrid mobile robot," *Robotics and Autonomous Systems*, vol. 133, Nov. 2020, doi: 10.1016/j.robot.2020.103627.

## BIOGRAPHIES OF AUTHORS



**Phuong Thao Thai**     is a lecturer at Hanoi University of Science and Technology. She is now working at the Department of Mechatronics, School of Mechanical Engineering. She completed 3 years of Ph.D. at Meiji University, Japan with the topic of origami technology. Her favorite topics are origami technology, dynamics, and controlling robot. She can be contacted at [thao.thaiphuong@hust.edu.vn](mailto:thao.thaiphuong@hust.edu.vn).



**Ngoc Hai Nguyen**     is a graduate of engineering degree from Hanoi University of Science and Technology. Currently, he is a Master of Science student in Mechatronics at School of Mechanical Engineering, Hanoi University of Science and Technology. His research interests are origami technology, dynamics, and control. He can be contacted at [nguyenngochai0511@gmail.com](mailto:nguyenngochai0511@gmail.com).